Brussels, Date 15th December 2014

Authors: Antonio Garcia-Uceda Juárez
Charles Hirsch

3rd International Workshop on Higher-Order CFD Methods

NUMECA Int., Chaussée de la Hulpe 189 Terhulpse Steenweg,
BE - 1170 Brussels, Belgium
Tel.: +32 (0)2 6478311, Fax.: +32 (0)2 6479398
www.numeca.com

1. Code description.

The results presented in this report have been obtained with a high-order Euler solver based on the novel Flux Reconstruction (FR) method (Huynh H.T. (2007)(2009)). This is implemented in the unstructured solver FINE/Open[tm], and handles every element topology (Hexas, Prisms, Tetras, and Pyrams) on hybrid meshes. In FR scheme the governing equations are solved in its differential form, thus no numerical integration is required as opposed to Discontinuous Galerkin (DG) methods.

The numerical solution $u(x)$ within each element is represented by a nodal basis that spans a polynomial space of order p. Solution values u_i that support this nodal basis are computed at defined locations within the reference element, being the degrees of freedom of the problem. These correspond to a 2D tensor product of Gauss points on Quad, and the so-called Williams-Shunn points in Williams D.M. (2013), on Trians. 3D elements Hexas and Prisms, respectively, are formed by tensor product with Gauss points in the 3rd dimension. A mapping $\mathbf{X}(\xi,\eta,\zeta)$ between the reference and real elements is constructed through isoparametric transformation. Curvilinear boundaries can be represented by Serendipity mapping, on both Hexas and Prisms, up to cubic order (see Zienkiewicz R.L. et al. (2005) for details).

In order to ensure consistency of the governing equations in differential form, a $C0$ continuous Flux function F(x) is constructed through the so-called correction functions (see Huynh H.T. (2007) for details), recovering a nodal-type DG scheme. These functions on Trians are computed following the approach in Huynh H.T. (2011). Resulting correction functions in 3D elements are the result of tensor product with the one “DG recovering” function in the 3rd direction. Explicit time integration is performed using a low-storage Runge-Kutta (RK) scheme of 4th order.

2. Case Summary.

The case presented is the C1.1: Transonic Ringleb Flow. Inlet conditions are imposed through total pressure, temperature and flow angle, all resulting from Ringleb exact solution with $q = 0.5$, and $k\epsilon[0.7, 1.5]$. Static pressure is imposed at the outlet, also resulting from Ringleb. Finally slip wall conditions are imposed on the lateral boundaries, with zero normal velocity.

Simulations are performed on four nested structured meshes of 12x4, 24x8, 48x16, and 92x32 Quad elements, and orders p=1,2,3. Third and fourth grids are shown in figure 1. On all boundaries, elements are curved by cubic Serendipity mapping, where two additional equispaced nodes on each boundary edge are mapped to the real geometry. Indeed it has been found that 2nd order mapping was not sufficient, resulting in spurious errors that eventually cause the solution to diverge.

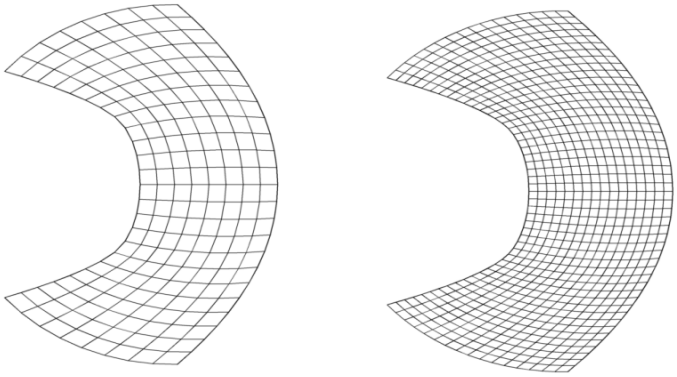

Figure 1: Meshes of 24x8 (left) and 48x16 (right) elements.

Simulations are started from the Ringleb exact solution throughout the flow domain. Convergence is assumed when the L2 norm of the continuity equation residual drop below 10^{-8}. The accuracy of the scheme is assessed through the computation of the L2 norm of the entropy error on the whole domain as follows:

$$\|e_{error}\| = \sqrt{\frac{\sum^{nbCell} \int \left(\frac{e - e_\infty}{e_\infty}\right)^2 dV}{\sum^{nbCell} V_i}}, \quad e = \frac{p}{\rho^\gamma}$$

Where integrals are calculated by a quadrature rule of sufficient order. The resulting values are plot against a characteristic length scale, and the slope gives the real order of accuracy of the scheme.

3. Results.

Solutions obtained on the meshes 24x8 and 48x16 are displayed in figures 2-6. Convergence has been reached only on grids 24x8, 48x16, and 92x32, and p=2,3. This is due to great sensitivity to geometrical accuracy. A fourth order Serendipity mapping on boundary elements might improve stability on coarser grids, but its implementation was not feasible due to time constraints.

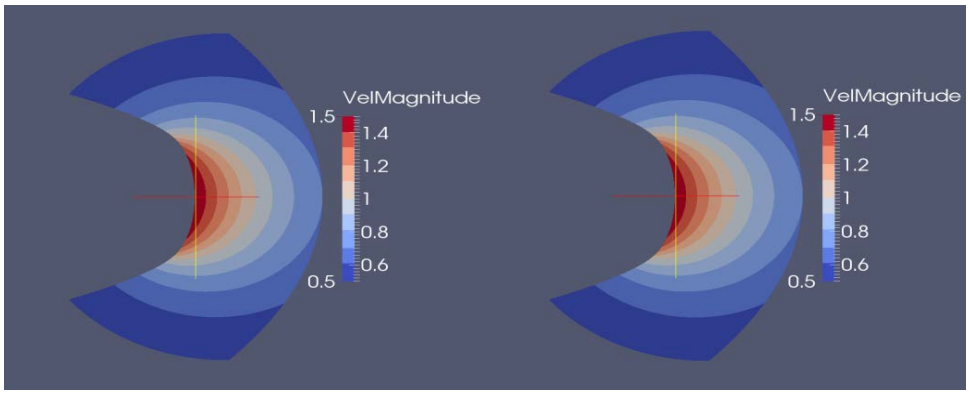

Figure 2: Contours of velocity q, on mesh of 24x8 elements, with p=2 (left), 3 (right).

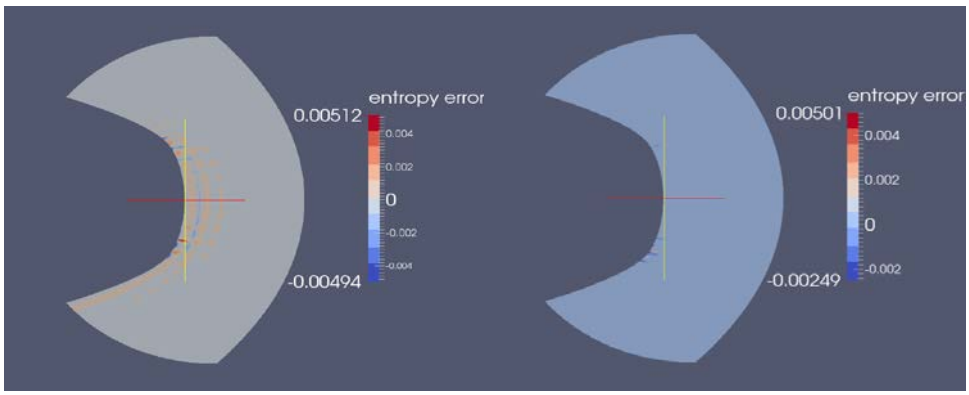

Figure 3: Contours of entropy error, on mesh of 24x8 elements, with p=2 (left), 3 (right).

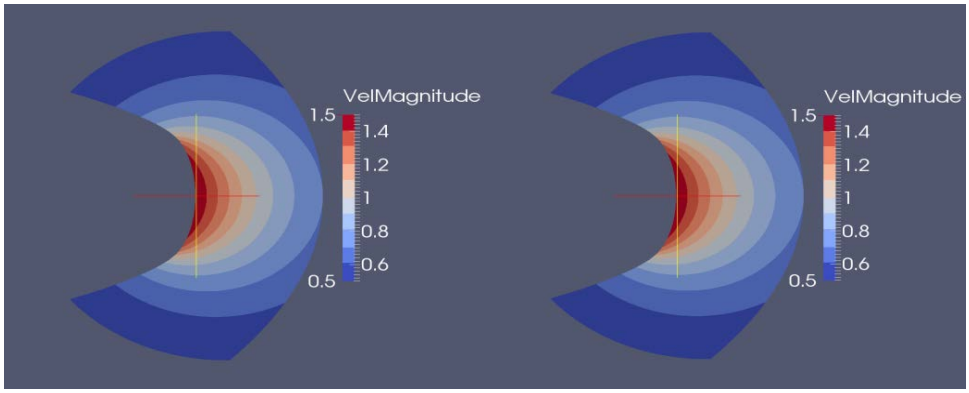

Figure 4: Contours of velocity q, on mesh of 48x16 elements, with p=2 (left), 3 (right).

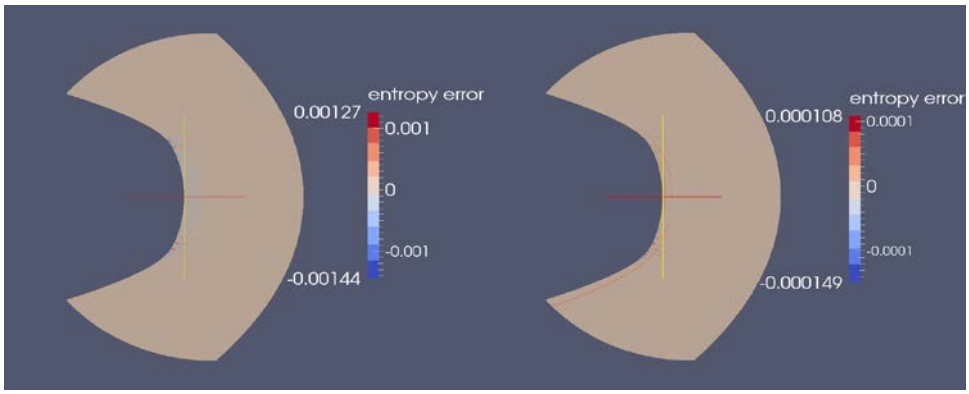

Figure 5: Contours of entropy error, on mesh of 48x16 elements, with p=2 (left), 3 (right).

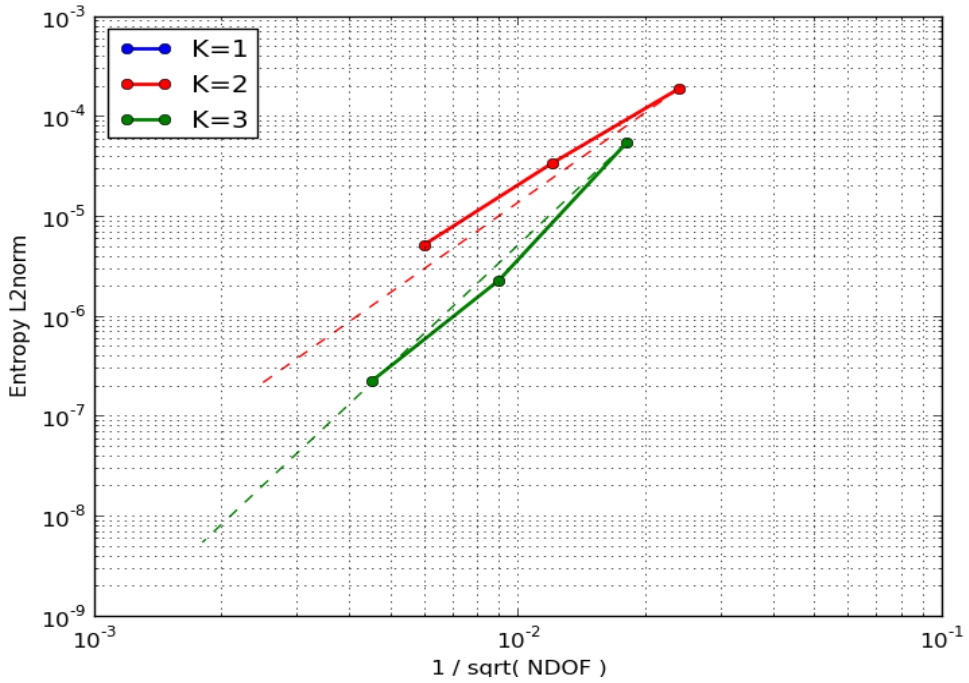

Figure 6: L2 norm of entropy error – characteristic length scale. Theoretical slope is displayed in dashed line.

Order p	Order of Accuracy
2	~2.6
3	~3.9

Table 1: Orders of accuracy resulting from figure 6. Values taken as the average between meshes 2-3 and 3-4.

Finally, figure 7 displays the L2 norm values of figure 6 against work units. Time is measured until convergence of 10^{-8} on continuity residuals is reached, account only for solve time. The Taubench reference time is 8.684 *s*, taken as average over 10 values to eliminate discrepancies.

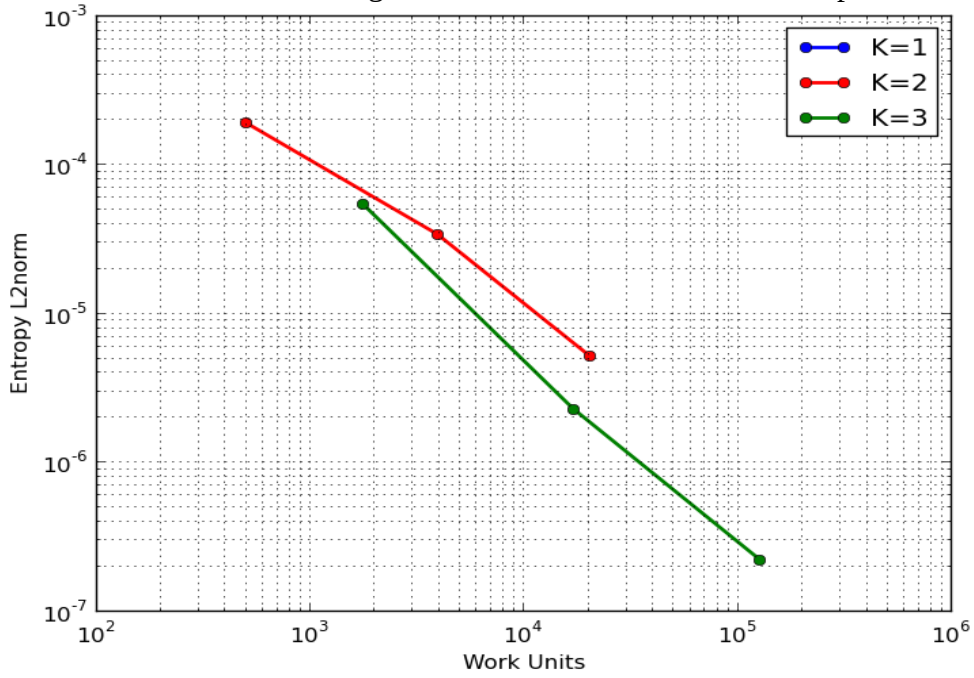

Figure 7: L2 norm of entropy error – work units. Taubench reference time: 8.684 s.

4. Conclusions.

Transonic Ringleb Flow is a very representative test case to validate a high-order Euler solver. Indeed, the transonic state will increment any inaccuracies due to insufficient mesh refinement, discretisation order, representation of boundaries, …, eventually causing the simulation to diverge. This way, a converged solution has only been achieved given a limit of h,p refinement: 3rd mesh onwards, and orders p=2,3, as well as providing cubic representation of curved boundaries.

The validation of the FR Euler solver has been demonstrated through this case. For the converged simulations, slopes computed in figure 6 match essentially the theoretical order of accuracy of every scheme. Discrepancies might be improved by means of 4th order discretisation of curved boundaries, which is not available in the FR solver. Finally, figure 7 demonstrates the correct scalability of the solver with the order p. However, times of computation are still very large, which suggest the need of a multigrid algorithm in order to accelerate convergence to steady state.

5. References.

Huynh H.T. (2007), A Flux Reconstruction Approach to High-Order Schemes Including Discontinuous Galerkin Methods. *AIAA Paper 2007-4079.*

Huynh H.T. (2009), A Reconstruction Approach to High-Order Schemes Including Discontinuous Galerkin for Diffusion. *AIAA Paper 2009-403.*

Huynh H.T. (2011), High-Order Methods Including Discontinuous Galerkin by Reconstuction on Triangular Meshes. *AIAA Paper 2011-44.*

Williams D.M. (2013), Energy-Stable High-Order Methods for Simulating Unsteady, Viscous, Compressible Flows on Unstructured Grids. *PhD thesiss, Stanford University*.

Zienkiewicz R.L., Taylor R.L., Zhu J.Z. (2005), The Finite Element Method: Its Basis and Fundamentals. *Elsevier, Butterworth Helneman.*